AIChE

Encapsulation of Nanoparticles by Polymerization Compounding in a Gas/Solid Fluidized Bed Reactor

Babak Esmaeili, Jamal Chaouki, and Charles Dubois
Dépt. de Génie Chimique, École Polytechnique de Montréal, C.P. 6079, Succ. Centre-Ville, Montréal, QC, H3C 3A7, Canada

DOI 10.1002/aic.11896
Published online July 23, 2009 in Wiley InterScience (www.interscience.wiley.com).

For the first time, a fluidized bed reactor was used for encapsulating nanoparticles by the polymerization compounding approach using Ziegler–Natta catalysts. The polymerization reaction was carried out using a solvent-free process in a gas-phase reactor. This direct gas–solid reaction greatly simplified collecting the particles of interest after polymerization because none of the extra steps often found in encapsulation processes, such as filtering and drying, were performed in this work. The grafting of the catalyst to the original surface of particles was confirmed by X-ray photoelectron spectroscopy. Micrographs obtained by transmission electron microscopy confirmed the presence of a thin layer of polymer, in the order of a few nanometers, around the particles. The thickness of this coating was affected by the operating conditions of the process. The characterization of the modified particles with electron microscopy also revealed that zirconia nanoparticles tend to be coated in an agglomerated state, whereas aluminum particles were mostly individually encapsulated by the polymer. In addition, the effects of temperature and pressure were studied on the encapsulation process and a kinetic analysis was presented based on the available models in the literature. *AIChE J, 55: 2271–2278, 2009*
Keywords: nanoparticles, encapsulation, fluidized bed, polymerization compounding

Introduction

Coating or encapsulating nanoparticles with polymers is desired in many applications to improve their chemical stability, reduce their toxicity, and facilitate their storage, transport, and processing. As two particular applications of nanoparticle coating, we specify the encapsulation of zirconia and aluminum nanoparticles. These nanoparticles are very promising materials in industrial applications. Over the last few years, the introduction of zirconium oxide-based ceramics into the field of dentistry has been greatly appreciated. In fact, dentures made from these materials have the required hardness and aesthetic qualities. Their production, however, poses serious cost-effectiveness problems mainly because of their ultra hard mechanical property. One solution to eliminate this difficulty is to coat the nanoparticles with a polymer using polymerization compounding (PC), followed by manufacturing the coping in composite form to make dentures. Manufacturing must take into account the shrinkage that occurs during densification. Finally, the composite denture is densified to sublime the polymer and obtain it in ceramic form. Figure 1 shows the compounds corresponding to the different steps mentioned earlier.

On the other hand, ultra fine aluminum powder is being recognized as a good candidate for diverse combustion applications, such as additives in solid rocket propellants and metallic fuel in explosive formulations. The aluminum nanoparticles have been reported to show burning rates 5–10 times greater than microsized ones and when used in gas generator fuels, they achieve a more complete combustion. These enhanced properties are due to their large specific surface per unit mass. However, the large specific surface area,

Correspondence concerning this article should be addressed to J. Chaouki at jamal.chaouki@polymtl.ca

Figure 1. From left to right starting from the top: composite ingot, composite coping, densified coping, and three false teeth ready to be implanted into the mouth.

[Color figure can be viewed in the online issue, which is available at www.interscience.wiley.com.]

which provides these powders with a high reactivity, makes them particularly difficult to maintain in an unoxidized state. Consequently, coating these powders with a polymer would be a solution to protect them from a nondesirable reaction, such as oxidation. As mentioned earlier, the application of this process is not limited to the applications mentioned for zirconia and aluminum. It can be applied to different types of nanoparticles to protect their surface, reduce their toxicity and facilitate their processing.

PC[1–4] is a technique that provides the modified particles or fibers with the properties required to obtain high-performance composite and nanocomposite materials. In this approach, the particle surface becomes involved in the polymerization reaction so that a very intimate contact between the particle surface and polymer can be established bringing improved interfacial properties and, consequently, enhanced properties of the nanocomposite.[5–7] In the last two decades, PC has been successfully applied to encapsulate different types of nanoparticles such as aluminum,[8] aluminum oxide,[9] zirconium oxide,[10,11] fumed silica,[12] silicon carbide,[13] and iron oxide[14] and nearly all reported experimental investigations were performed in the liquid phase. The ubiquity of the slurry-based process is easily explained. First, most of the monomers of interest are either readily available in a liquid state at room temperature or very soluble in common organic solvents. Therefore, a liquid phase process is intrinsically compatible with the nature of the reagents. Second, the liquid medium provides the appropriate conditions to disperse agglomerates and clusters in finer particles to have them individually coated. However, the results showed that this is not completely successful and the coating of agglomerates has always occurred together with the encapsulation of individual particles.[11] Third, the success of the coating process requires that a very small quantity of catalyst or initiator be deposited on a relatively large surface of particles. For example, in the case of ethylene polymerization, a small amount of Ziegler–Natta catalyst, around 1 μl, must be placed on a square meter of particle surface to be coated. Therefore, by dissolving that small amount of catalyst in an organic solvent, where particles have already been dispersed, it is easier to achieve a uniform activation of the particle surface before the polymerization reaction.

Some drawbacks, however, arise when the process is carried out in liquid phase, as the polymerization reaction must be followed by additional steps to isolate the coated particles.[8] After encapsulation, the reaction slurry must be filtered to separate the coated particles from the solvent. This step is usually accompanied by washing the encapsulated powders to eliminate solvent impurities, catalyst and the nonreacted monomers. Then, the coated particles must be completely dried in an oven overnight. Subsequently, the dried particles form a hard bulk material, which needs to be grinded to obtain finely coated particles. To accomplish all of the aforementioned additional processes requires more than the polymerization reaction time itself, which usually extends only over a few minutes. Accordingly, the encapsulation process costs for a liquid–solid reaction, particularly when dealing with large amounts of particles, are significant. In addition, under these conditions, it is difficult to ensure a complete removal of the impurities in the solvent and to obtain the desired particle size by grinding the bulk material recovered from the process.

An evident alternative to eliminate all the aforementioned negative aspects is to perform the nanoparticle encapsulation as a gas–solid reaction, where the gaseous phase contains the monomer of interest. The polymerization of ethylene via Ziegler–Natta catalyst for nanoparticle encapsulation and composite preparation has been reported by several researchers,[8,15,16] using a liquid suspension where the ethylene gas is dissolved. We also have successfully used this procedure to encapsulate zirconia nanoparticles in hexane.[11] The work reported in this article was aimed at extending the previously described slurry-based process to a gas phase reaction using a fluidized bed reactor. For this purpose, two different types of nanoparticles, zirconia and aluminum, were considered for encapsulation studies by polyethylene via the Ziegler–Natta polymerization scheme. This simplified process is performed free from solvent impurities (particularly water) and no extra separation steps, such as filtering, washing, drying, and grinding, are required to collect the coated nanoparticles after the polymerization reaction. To the best of our knowledge, this original work by our group is being accomplished for the first time. It should be mentioned that although this system, in some aspects, is similar to the processes dealing with ethylene homopolymerization using the Ziegler–Natta catalyst, there are some major differences in these two processes. In our case, the polymerization occurs on the surface of nanoparticles, whereas in the homopolymerization of ethylene, the substrate that supports the polymerization catalyst has a characteristic length in the micrometer range. In addition, the amount of catalyst, when performing nanoparticle encapsulation, is limited by the active sites on the surface of nanoparticles. Besides, the pressure in the ethylene homopolymerization process may rise very high, whereas the pressure used in the nanoparticle encapsulation studies was moderate, and in some instances, close to the ambient pressure.

The major difficulty associated with taking this reaction from a liquid to a gas phase process was to attach the

Table 1. Physical Properties of Zirconia and Aluminum Particles

	Al (TEKNA)	ZrO_2 (Aldrich)
Average diameter (nm)	120	250
Specific surface area (m^2/g)	16.5	5.5
Solid density (kg/m^3)	2700	5900
Bulk density (kg/m^3)	350	1200

Ziegler–Natta catalyst to the surface of the particle. The approach investigated consisted of evaporating the Ziegler–Natta catalyst before it entered the fluidized bed reactor, and then condensing the resulting vapor on the particle surface in the reactor. As there is no thermal gradient in the reactor, all particles having the same temperature due to the mixing action of the fluidization process,[17] the catalyst vapors uniformly deposit on the particle surface. Therefore, it would be anticipated that the polymerization reaction is uniformly applied on the particles.

Experimental

Materials

Zirconia powder purchased from Sigma-Aldrich and aluminum powder manufactured by TEKNA were used for the polymer coatings experiments. Table 1 reports some of the physical properties of these particulate materials.

Ethylene gas with a purity of 99.5%, supplied by Canadian liquid air was used as monomer for the polymerization reaction. The Ziegler–Natta catalyst system, consisting of titanium tetrachloride ($TiCl_4$), manufactured by Acros, as the catalyst, and triethylaluminum ($AlEt_3$) obtained from Sigma-Aldrich, as cocatalyst, was stored and handled in a glove box to protect them from moisture and oxygen. Methylaluminoxane (MAO) also purchased from Sigma-Aldrich was used to determine the hydroxyl groups density on particles surface.

Quantification of hydroxyl chemical groups on nanoparticles

The polymerization process used in this work necessitates the anchoring of the catalyst to the particles using the OH sites on their outer surface. Accordingly, appropriate amounts of the catalyst and cocatalyst need to be estimated from the OH group density on the nanoparticles surface. To carry out this quantification,[18] a small amount of nanoparticles, about 0.5 g, is agitated and heated in 5 ml of dry toluene in a laboratory test tube where a flow of dry nitrogen and vacuum conditions are first applied to remove oxygen and humidity from the system. After 1 h, the laboratory test tube is cooled to ambient temperature, and subsequently, 1 ml of MAO is injected into the closed tube through a septum. As a result of the reaction between each mole of MAO and hydroxyl groups of the surface, one mole of methane is released. Consequently, the hydroxyl group density is calculated by determining the methane gas evolved in the process using a pressure monitoring setup. An example of the use of the observed pressure rise to determine the minimum amount of catalyst and cocatalyst is given in Table 2. It should be mentioned that the amount of catalyst and cocatalyst used in all the reactions were in excess of 100%.

Table 2. Catalyst and Cocatalyst Calculated Based on OH Concentration

	Aluminum	Zirconia
Pressure rise	142.5 mm Hg/g	50.7 mm Hg/g
OH concentration on particles	5.4×10^{-4} mol/g	1.9×10^{-4} mol/g
$TiCl_4$ (pure catalyst)	0.06 ml/g	0.02 ml/g
$AlEt_3$ (1 M solution in hexane)	0.54 ml/g	0.19 ml/g

By converting the values for OH concentration on aluminum and zirconia particles to OH molecules per square nanometer using the specific surface area given in Table 1, around 20 OH/nm^2 are evaluated on the nanoparticles surfaces. On the other hand, by considering the OH molecule diameter of 5 Å and OH concentration on alumina nanoparticles reported in the literature,[19] it is concluded that the OH molecules on particle surface should not exceed five over square nanometer. We do not have a good explanation for this over prediction. It might be because of the possible reactions between MAO and other groups in toluene and/or on particles. However, as mentioned earlier, the catalyst was injected in excess for encapsulation experiments and therefore, there is no impact on the work by introducing more excess of catalyst because nonreacted catalyst exit the reactor via carrying gas.

Synthesis

Figure 2 illustrates the encapsulation process of nanoparticles in a fluidized bed reactor. The reactor itself used for this work was a simple cylinder made of stainless steel 2 cm in diameter and 3 cm in height. Gas was introduced into the bed through a porous plate with a 5 μm pore size to provide a homogenous fluidization of particles. The reaction proceeds as follows: First, nitrogen gas, passed through an electrical heater, provides sufficient energy to heat the entire system so that the injection point attains a higher temperature than the boiling temperature of the catalyst. A second electrical heater was also located around the fluidized bed to adjust the reactor temperature at the desired reaction temperature. Then, the catalyst and, after a few minutes, the cocatalyst are injected into the system. As the temperature at the injection point is higher than the boiling temperature of $TiCl_4$ and $AlEt_3$, the catalyst and cocatalyst evaporate and enter the reactor in the gas phase. Subsequently, the catalyst

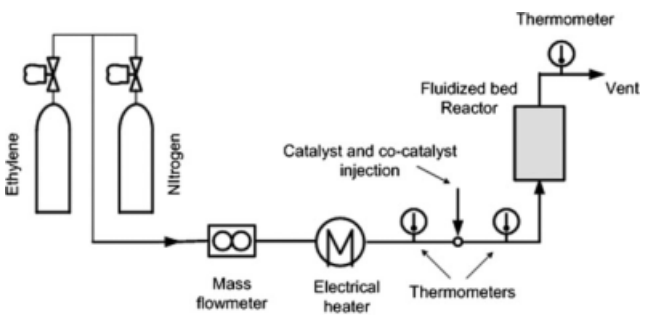

Figure 2. Schematic of the encapsulation of nanoparticles in fluidized bed reactor.

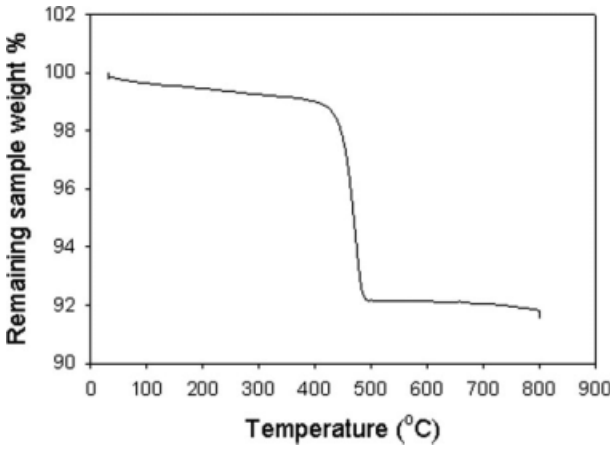

Figure 3. TGA graph of zirconia coated nanoparticles (reaction conditions: T = 65°C, P = 210 kPa).

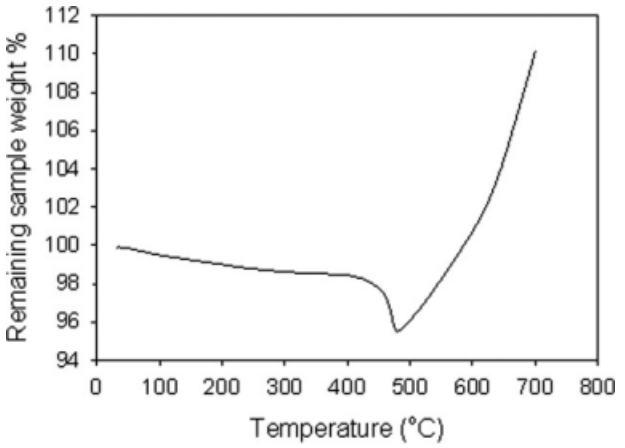

Figure 4. TGA graph of aluminum coated nanoparticles (reaction conditions: T = 72°C, P = 140 kPa).

and cocatalyst vapors uniformly condense on nanoparticles in the reactor, where temperature is lower than catalyst and cocatalyst boiling points. After the catalyst grafting step on the particles, the polymerization reaction was started by switching from nitrogen to ethylene as the fluidizing gas. After the desired reaction time, ethylene flow was stopped and the system was flushed with nitrogen. The gas velocity in the reactor for aluminum and zirconia was 5 and 10 cm/s, respectively, which are much higher than minimum fluidization velocity of these powders.[17] The temperature and the pressure in the reactor were kept constant for a given reaction, and varied within range of 65–75°C and 140–280 kPa, respectively, during the series of runs in this study.

Characterization

The amount of polymer on the zirconia particles was determined by thermogravimetry analysis (TGA) using a TA instruments 500 apparatus operated in a 25–800°C temperature range at a 10°C/min heating rate under a flow of nitrogen. The thickness of the polymer layer on the surface of nanoparticles was observed using Jeol JEM-2100F transmission electron microscope (TEM). X-ray photoelectron spectroscopy (XPS) was used to study the interface of the grafted polymer and the original surface of particles.

Results and Discussion

A typical TGA of coated zirconia and aluminum nanoparticles is presented in Figures 3 and 4. One can see that a sharp weight loss appears at 450–500°C corresponding to the pyrolysis of high-molecular weight polyethylene (HMWPE). This confirms the presence of HMWPE on the surface of nanoparticles.

It can be seen that in the TGA graph of aluminum, a weight increase occurs after polyethylene degradation at around 500°C. It could be because of adsorption of nitrogen on aluminum surface, and also, the oxidation reaction. After polymer degradation, the surface of nanoparticles becomes reactive, and therefore, it can react with the traces of oxygen found in the nitrogen gas leading to a weight increase in the TGA plot.

The characterization of the coated particles was continued by the verification of catalyst grafting on the nanoparticles surface using XPS, as reported in Figure 5. It should be noted that to show the results of the original and coated particles in the same graph, the spectrum corresponding to coated particles is shifted by 50,000 counts/s. However, the original data obtained from the software are reported in Table 3. As shown in Figure 5, titanium and chlorine peaks can be clearly observed at a binding energy of 458 and 199 eV, respectively, corresponding to Ziegler–Natta catalyst in coated aluminum.

In addition, as we previously mentioned,[11] by comparing XPS results of the coated particles with different polymer contents, it is confirmed that the catalyst is only found at the polymer-substrate interface, indicating that polymerization reaction can be initiated only from the original surface of particles. It was proposed that Ziegler–Natta catalyst, $TiCl_4$, reacts with hydroxyl groups on particles surface as shown in following equation,

$$-OH + TiCl_4 \rightarrow -O-TiCl_3 + HCl \qquad (1)$$

Therefore, there is a covalent bond established between the catalyst and the particles, and as a result, the

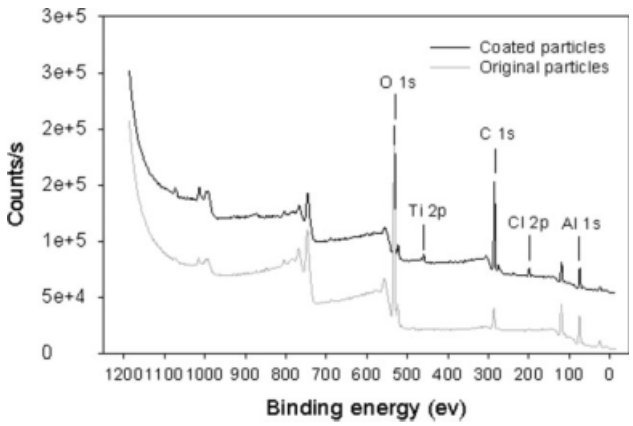

Figure 5. XPS graphs of original and coated aluminum nanoparticles.

Table 3. Elemental ID and Quantification for Original and Coated Aluminum Nanoparticles

Name	Peak BE	Height (Original) (cps)	Area (*p*) (Original) (cps eV)	Height (Coated) (cps)	Area (*p*) (Coated) (cps eV)	Atom % (Original)	Atom % (Coated)
Al 1s	74	22804.00	110210.15	15132.88	65809.97	26.59	3.46
O 1s	532	139198.88	657310.45	99992.92	428450.91	55.82	42.82
C 1s	285	17081.89	90798.42	59493.24	235550.63	17.59	53.72

polymerization starts from the surface of the particles, which favors their encapsulation. Although the chain transfer termination usually occurs in Ziegler–Natta polymerization systems, a favorable interaction is established between the polymer and substrate. As the polymerization reaction starts from the substrate and monomers are consecutively added to polymer chains, the diffusional limitations and steric hindrance effects are significantly lower than in the case where polymer chains are simply brought to the surface by the substrate nucleating action. Therefore, appropriate wetting of the solid surface by the polymer, and consequently, high-interfacial interactions are achieved. As shown in Table 3, the relative intensity of aluminum and oxygen peaks, representing the original surface of particles, is significantly reduced after polymerization. In addition, the relative intensity of carbon peak, associated with the presence of a hydrocarbon based polymer coating, increased considerably after the polymerization in comparison with original particles. It can be seen that the weight percentage of aluminum and oxygen elements was reduced from 26.59 and 55.82% for noncoated particles to 3.46 and 42.82% for coated particles. In contrast, carbon content increases from 17.59% for noncoated particles to 53.72% for coated particles. The initial amount of carbon for noncoated particles, detected by XPS, is due to the sample contamination by atmospheric carbon (CO_2). Similar results were obtained for zirconia nanoparticles.

It should be mentioned that the surface of pure aluminum particles is very reactive and very sensitive to oxygen; therefore, it is oxidized rapidly when exposing to air. As a result, a thin layer of aluminum oxide around 2 nm has been already formed around aluminum nanoparticles before coating. As XPS apparatus applied in this work was able to detect and analyze the depth of about 6 nm from the free surface of particles and, by considering the thickness of polymer layer which is about 4 nm as shown in next paragraph, the XPS apparatus detected mostly the polymer coat and aluminum oxide layer, which leads to evaluate relatively high-oxygen content for encapsulated particles.

TEM observations carried out on original and coated aluminum and zirconia nanoparticles are presented in Figures 6 and 7, respectively. As shown in Figure 6a and 7a, the surface of noncoated particles possesses a sharp edge and no other phase is distinguished. On the other hand, as shown in Figure 6b for a coated aluminum particle, an image contrast is found that corresponds to a polyethylene layer of about 4 nm thick uniformly applied around the particles. One can see in Figure 7b that zirconia particle was covered by a polymer layer around 5 nm; however, it is observed that the polymer layer on zirconia particles is not uniform in comparison with that on aluminum. In addition, zirconia particles tend to be coated in a more agglomerated state as observed in Figure 8, whereas, aluminum powders were individually encapsulated.

These results are consistent with the results obtained in our previous work.[17] It was mentioned that the fluidization of zirconia and aluminum occurs in agglomerate state as shown in Figure 9. It was also observed that the minimum fluidization velocities of zirconia and aluminum are 2.3 and 0.25 cm/s, respectively. These values are much higher than minimum fluidization velocity of individual nanoparticles calculated by available correlations.[20] It means that zirconia and aluminum nanoparticles fluidize as clusters of particles. In addition, we observed that the agglomerates in the bed of zirconia are larger compared with those found in the bed of aluminum. Therefore, the agglomerate coating is inevitable when encapsulating nanoparticles, particularly zirconia nanoparticles.

According to the experiments,[17] it was understood that by increasing the gas velocity, large agglomerates are broken to smaller ones due to higher drag force in higher gas velocities. Therefore, in the range of gas velocity where we did

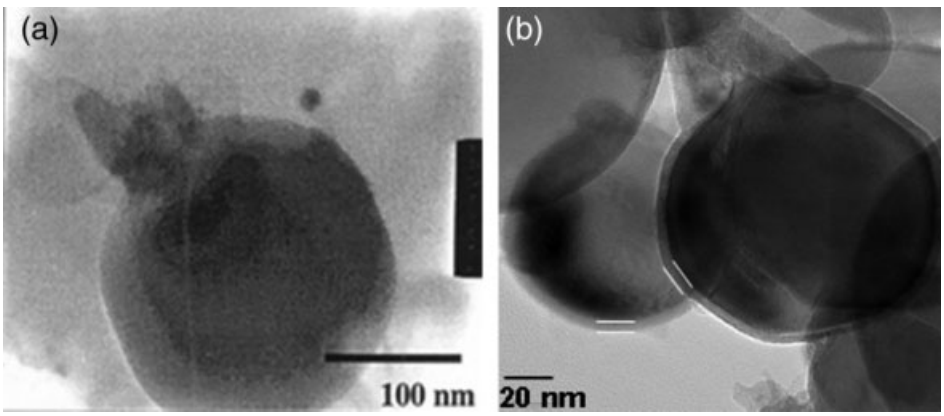

Figure 6. TEM images of (a) original and (b) coated aluminum nanoparticles.

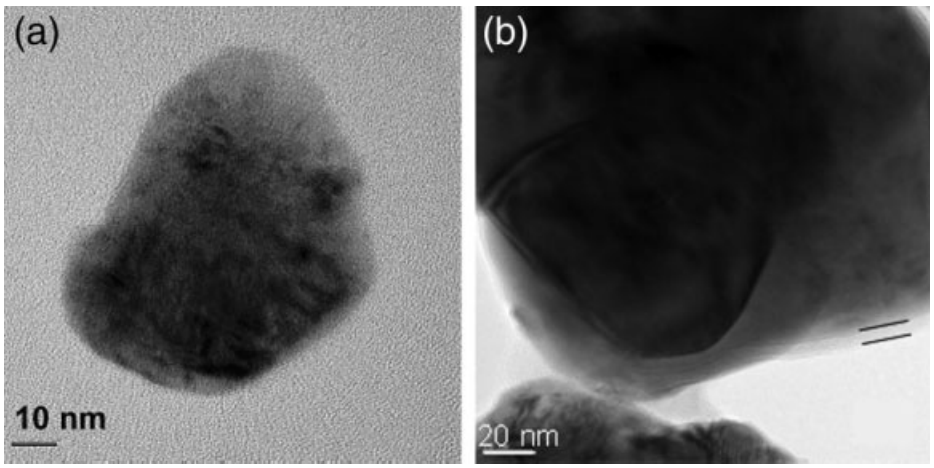

Figure 7. TEM images of (a) original and (b) coated zirconia nanoparticles.

the fluidization experiments, the agglomerate size are smaller for higher gas velocity for a given particle type.

The effects of polymerization conditions

The encapsulation of zirconia nanoparticles was carried out under different process conditions as listed in Table 4. The encapsulation time was around 12 min for all runs except for trial number 4, in which the flow of monomer was stopped after 6 min. It can be seen that the temperature and pressure have considerable effects on polymerization process. From Run No. 1 and 2, it is observed that by increasing the pressure from 140 to 210 kPa, the polymer content increases by 5%. At 75°C, the polymer quantity increases by 5.5% by increasing the pressure from 140 kPa in Run 3 to 280 kPa in Run 4, where the reaction time was only half that used in the low pressure reaction. By comparing Run No.1 and No.3, a 5.5% increase in polymer content is realized by increasing the temperature from 65 to 75°C. The corresponding TGA graphs are presented in Figure 10.

Kissin et al. studied the kinetic of ethylene homopolymerization with the heterogeneous Ti-based Ziegler–Natta catalyst.[21] They found that the overall rate of ethylene homopolymerization has the reaction order n with respect to the ethylene concentration, C_E,

$$R_{pol} = k_{eff} C_E^n \tag{2}$$

The order of reaction, n, was evaluated as 1.77 where the polymerization reaction is carried out in the gas phase. The effective rate constant, k_{eff}, is the product of the propagation rate constant, k_p, and the concentration of active centers, C^*.

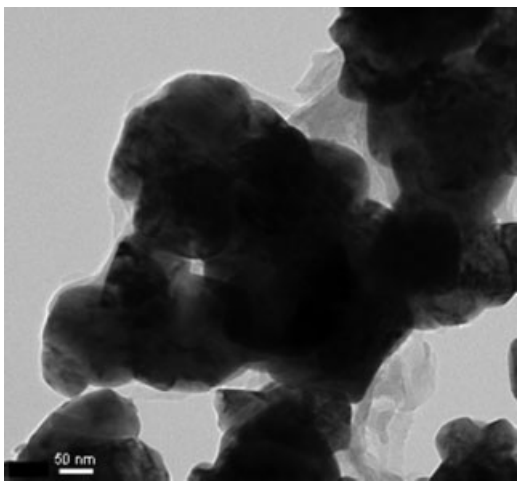

Figure 8. TEM image of coated agglomerate of zirconia nanoparticles.

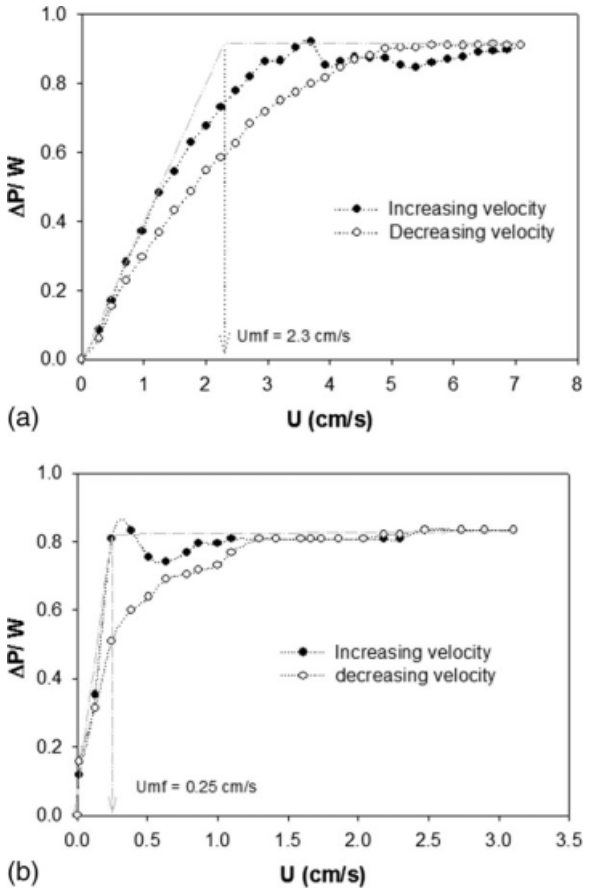

Figure 9. Minimum fluidization velocities for (a) zirconia and (b) aluminum nanoparticles.

Table 4. Different Process Conditions for Zirconia Nanoparticles Encapsulation

Operation No.	Temperature (°C)	Pressure (kPa)	Polymer Content (%)
1	65	140	2
2	65	210	7
3	75	140	7.5
4	75	280	13

If the propagation rate is assumed to be temperature dependant according to the Arrhenius equation, then the overall polymerization rate can be written as the following equation:

$$R_{\text{pol}} = C^* k_{\text{p0}} \exp\left(\frac{-E}{RT}\right) C_{\text{E}}^n \tag{3}$$

where E is the activation energy for the propagation.

In an investigation on ethylene polymerization kinetic with a heterogeneous metallocene catalyst, Bergstra and Weickert evaluated C^*k_{p0} and E as 2.49×10^{10} m^3/(h gcat) and 74.9 kJ/mol.[22] By applying these values in the reaction rate proposed by Kissin, the amount of polymer was significantly overestimated in comparison with our experimental data. Therefore, we used the same reaction kinetic and activation energy constant, and by using the experimental results provided in Table 4, the C^*k_{p0} was modified to 3.3×10^7 m^3/(h gcat). The results are given in Table 5.

The experimental polymer mass is presented based on 1 g of zirconia nanoparticles. As shown in the table, the values obtained by the kinetic model using the modified C^*k_{p0} are in agreement with the experimental results. Therefore, the model presented by Kissin for ethylene homopolymerization is valid for nanoparticle encapsulation by polyethylene using PC. On the other hand, there is a great difference between C^*k_{p0} presented in the work of Bergstra and Weickert and the one modified in this work. There would be two explanations for this difference. First, C^*k_{p0} in the work of Bergstra and Weickert has been obtained for the ethylene polymerization using metallocene catalyst, which is more reactive than Ziegler–Natta catalyst. The second reason is related to the concentration of active centers on the supports. Although in this research, the catalyst injected into the reactor corresponds to the hydroxyl group on nanoparticles, it is expected that a part of the injected catalyst was not deposited on the nanoparticles due to particle agglomeration, as shown in Figure 8. Therefore, it seems that the concentrations of active centers available for polymerization reaction are much lower than those in the ethylene homopolymerization process.

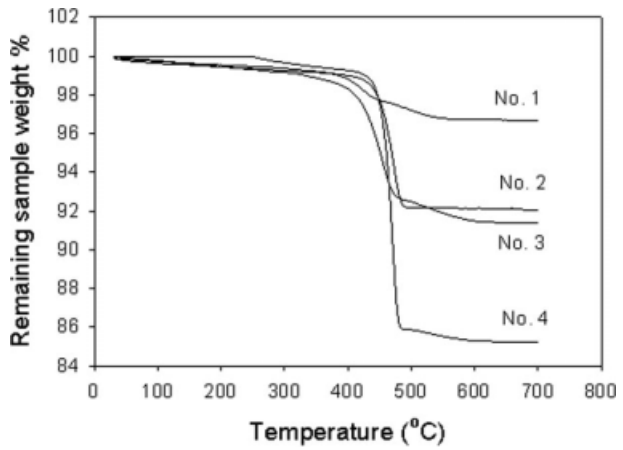

Figure 10. TGA graphs of zirconia encapsulation in different operations.

Table 5. Comparison Between Experimental Data and Calculated Polymer Amount Using the Kinetic in the Literature

Operation No.	Temperature (°C)	Pressure (kPa)	Polymer Quantity (Experimental) (g)	Polymer Quantity (Calculated) (g)
1	65	140	0.020	0.033
2	65	210	0.070	0.067
3	75	140	0.075	0.067
4	75	280	0.130	0.115

A comparison between nanoparticle encapsulation in slurry and fluidized bed reactors

The TEM images of coated agglomerates of zirconia produced by the slurry[11] and the gas/solid fluidized bed reactor processes are presented in Figure 11. As the images show, the agglomerate in the slurry phase reactor is smaller than those in the fluidized bed reactor. As in the slurry phase reactor, the particles are dispersed in the solvent by agitation and ultrasound, the large agglomerates are broken into smaller ones and even individual particles, whereas in the fluidized bed reactor used in this work, no external force was applied. The agglomerates in the fluidized bed reactor are therefore larger than those in the slurry phase reactor. If an external force, such as vibration, were applied to the fluidized bed reactor, the agglomerate sizes and the risk of agglomerate coating could be reduced. However, the encapsulation process in the slurry phase must be followed by additional steps, such as filtering, drying, and grinding to isolate the coated particles. Accomplishing all of the aforementioned additional processes requires much more than the polymerization reaction time itself. Accordingly, the encapsulation process cost more for a liquid–solid reaction, particularly when dealing with large amounts of particles. In addition, under these conditions, it is difficult to ensure a complete removal of the impurities in the solvent.

Conclusions

It was shown that a fluidized bed reactor could be used for encapsulating nanoparticles via the PC approach. In this work, a Ziegler–Natta catalyst was used to polymerize ethylene to encapsulate aluminum and zirconia nanoparticles in the gas phase. Thermogravimetry results showed that particles were coated by a high-molecular weight polyethylene. The grafting of polyethylene on the particle surface was further confirmed by XPS results verifying that the polymerization reaction started only from the substrate, which leads to a uniform polymer layer applied around the nanoparticles. As observed from electron microscopy images, the process is capable of coating individual particles with a polymer film a few nanometers in thickness. However, in the case of

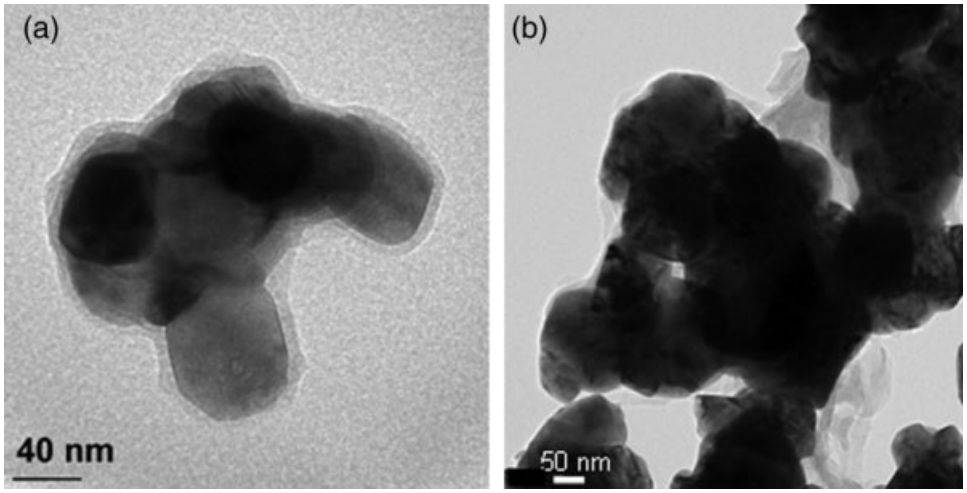

Figure 11. Coated agglomerates of zirconia in (a) the slurry phase and (b) in the fluidized bed reactors.

zirconia, it was also revealed that some agglomerates were encapsulated by the polymer, which is obviously not desirable. It was found that even under the mild process conditions used, the temperature and pressure have a considerable effect on the polymerization reaction and, hence, on polymer content on the coated particles. Therefore, the process of nanoparticle encapsulation can easily be controlled by adjusting the operating conditions. By comparing the encapsulation process in the slurry phase and fluidized bed reactor, it is understood that the size of agglomerates in the fluidized bed reactor are larger than those in the slurry phase, which leads to larger coated agglomerates in the former. On the other hand, there is no solvent used in the fluidized bed reactor. Therefore, coated particles are easily collected immediately after encapsulation without performing any additional process, such as filtering or drying, which are required when performing the process in a slurry phase reactor.

Literature Cited

1. Wang Q, Kaliaguine S, Ait-Kadi A. Catalytic grafting: a new technique for polymer-fiber composites. I. Polyethylene-asbestos composites. *J Appl Polym Sci*. 1992;44:1107–1119.
2. Wang Q, Kaliaguine S, Ait-Kadi A. Catalytic grafting—a new technique for polymer fiber composites. III. Polyethylene-plasma-treated Kevlar fibers composites. *J Appl Polym Sci*. 1993;48:121–136.
3. Salehi-Mobarakeh H, Brisson J, Ait-Kadi A. Interfacial polycondesation of nylon-6,6 at the glass fibre surface and its effect on fibre-matrix adhesion. *J Mater Sci*. 1997;32:1297–1304.
4. Salehi-Mobarakeh H, Brisson J, Ait-Kadi A. Ionic interphase of glass fiber/polyamide 6,6 composites. *Polym Compos*. 1998;19:264–274.
5. Kasseh A, Ait-Kadi A, Riedl B, Pierson JF. Organic/inorganic hybrid composites prepared by polymerization compounding and controlled free radical polymerization. *Polymer*. 2003;44:1367–1375.
6. Shin SYA, Simon LC, Soares JBP, Scholz G. Polyethylene-clay hybrid nanocomposites: in situ polymerization using bifunctional organic modifiers. *Polymer*. 2003;44:5317–5321.
7. Wang Y, Pei X, Yuan K. Reverse ATRP grafting from silica surface to prepare well-defined organic/inorganic hybrid nanocomposite. *Mater Lett*. 2005;59:520–523.
8. Roy C, Dubois C, Lafleur P, Brousseau P. The dispersion and polymer coating of ultrafine aluminum powders by the Ziegler Natta reaction. *Mater Res Soc Symp Proc*. 2004;800:AA2.5–AA2.5.6.
9. Shi D, Wang SX, van Ooij WL, Wang LM, Zhao J, Yu Z. Uniform deposition of ultrathin polymer films on the surfaces of Al_2O_3 nanoparticles by a plasma treatment. *Appl Phys Lett*. 2001;78:1243–1245.
10. Rovira-Bru M, Giralt F, Cohen Y. Protein adsorption onto zirconia modified with terminally grafted polyvinylpyrolidone. *J Colloid Interface Sci*. 2001;235:70–79.
11. Esmaeili B, Chaouki J, Dubois C. Polymerization compounding on the surface of zirconia nanoparticles. *Macromol Symp*. 2006;243:268–276.
12. Dubois C, Rajabian M, Rodrigue D. Polymerization compounding of polyurethane-fumed silica composites. *Polym Eng Sci*. 2006;46:360–371.
13. Che J, Wang X, Xiao Y, Wu X, Zhou L, Yuan W. Effect of inorganic-organic composite coating on the dispersion of silicon carbide nanoparticles in non-aqueous medium. *Nanotechnology*. 2007;18:1–6.
14. Garcia I, Tercjak A, Zafeiropoulos NE, Stamm M, Mondragon I. Generation of core/shell iron oxide magnetic nanoparticles with polystyrene brushes by atom transfer radical polymerization. *J Polym Sci Part A: Polym Chem*. 2007;45:4744–4570.
15. Rajabian M, Dubois C. Polymerization compounding of HDPE/Kevlar composites. I. Morphology and mechanical properties. *Polym Compos*. 2006;27:129–137.
16. Zhang X, Simon LC. In situ polymerization of hybrid polyethylene-alumina nanocomposites. *Macromol Mater Eng*. 2005;290:573–583.
17. Esmaeili B, Chaouki J, Dubois C. An evaluation of the solid hold-up distribution in a fluidized bed of nanoparticles using radioactive densitometry and fiber optics. *Can J Chem Eng*. 2008;86:543–552.
18. Sato M, Norio Kobayashi TK, Shima Y. Hydroxyl groups on silica, alumina, and silica-alumina catalysts. *J Catal*. 1967;7:342–351.
19. Rong MZ, Ji QL, Zhang MQ, Friedrich K. Graft polymerization of vinyl monomers onto nanosized alumina particles. *Eur Polym J*. 2002;38:1573–1582.
20. Kunii D, Levenspiel O. *Fluidization Engineering*, 2nd ed. Boston: Butterworth-Heinemann, 1991.
21. Kissin YV, Mink RI, Nowlin TE. Ethylene polymerization reactions with Ziegler-Natta catalysts. I. Ethylene polymerization kinetics and kinetic mechanism. *J Polym Sci*. 1999;37:4255–4272.
22. Bergstra MF, Weickert G. Ethylene polymerization kinetics with a heterogeneous metallocene catalyst—comparison of gas and slurry phases. *Macromol Mater Eng*. 2005;290:610–620.

Manuscript received Apr. 24, 2008, and revision received Feb. 4, 2009.